ARTICLE

# Assessing elastic property and solid-solution strengthening of binary Ni–Co, Ni–Cr, and ternary Ni–Co–Cr alloys from first-principles theory

Zhi-biao Yang and Jian Sun[a)]
*Shanghai Key Laboratory of Advanced High-Temperature Materials and Precision Forming, School of Materials Science and Engineering, Shanghai Jiao Tong University, Shanghai 200240, People's Republic of China*

Song Lu
*Applied Materials Physics, Department of Materials Science and Engineering, Royal Institute of Technology, Stockholm SE-100 44, Sweden*

Levente Vitos
*Applied Materials Physics, Department of Materials Science and Engineering, Royal Institute of Technology, Stockholm SE-100 44, Sweden; Division of Materials Theory, Department of Physics and Materials Science, Uppsala University, Uppsala SE-75120, Sweden; and Research Institute for Solid State Physics and Optics, Wigner Research Center for Physics, Budapest H-1525, Hungary*

(Received 31 January 2018; accepted 11 May 2018)

The elastic properties and solid-solution strengthening (SSS) of the binary Ni–Co and Ni–Cr, and ternary Ni–Co–Cr alloys were investigated by the first-principles method. The results show that both Co and Cr increase lattice parameters of the binary alloys linearly. However, nonlinearity is found in compositional dependence of lattice parameters in the ternary Ni–Co–Cr alloys, that is, Co increases but decreases the lattice parameter at low and high Cr concentrations, respectively. Co increases the bulk, shear, and Young's moduli (*B*, *G*, and *E*), while Cr increases *B* but decreases *G* and *E* in the binary alloys. In the ternary Ni–Co–Cr alloys, *G* and *E* have a similar compositional dependence to those in the binary alloys, except for *B*. Based on the Labusch model, the SSS parameter of Ni–Cr is larger than that of Ni–Co. The SSS effect increases significantly with Cr addition, especially at low Co concentrations in the ternary Ni–Co–Cr alloys. Meanwhile, it increases mildly with Co addition at low Cr concentrations but decreases with Co addition at high Cr concentrations.

## I. INTRODUCTION

Ni-based superalloys are widely used in aero-engines due to their excellent mechanical properties and oxidation resistance at high temperatures.[1,2] The phase of superalloys comprises a face-centered cubic (fcc) Ni-rich solid solution (γ phase) strengthened by coherent particles of $L1_2$-ordered $Ni_3Al$ precipitates (γ′ phase). In a series of commercial Ni-based superalloys, such as Inconel 939, CMSX-4, TMW, and so on, Co and Cr are the main alloying elements, partitioning preferentially in the γ phase.[3–5] Additions of Co and Cr elements certainly produce solid-solution strengthening (SSS) for the γ phase in superalloys. Furthermore, Co is reported to increase the lattice misfit between the γ and γ′ phases and then enhances the high temperature strength and creep resistance of superalloys.[1] High concentrations of Cr element allow the formation of a continuous chromia ($Cr_2O_3$) scale with inherent sulfidation and oxidation resistance at high temperatures.[6]

SSS plays an essential role on mechanical properties of Ni-based superalloys, and it has been investigated theoretically and experimentally for the past several decades.[7–10] On the mechanism of SSS, it is commonly assumed that dislocations move through the solvent lattice and are impeded by the solute atoms, contributing to the strength of the alloys. The general way to assess SSS is the linear elasticity theory, in which the two important strengthening parameters are atomic and elastic misfit parameters, respectively. The classic Fleischer model treats the interaction of dislocations with strong pinning solute atoms on the gliding plane, giving rise to the square-root-power dependence of strengthening on the solute concentration, which applies to the dilute solid solutions.[11] The statistical theory proposed by Labusch models the interaction of gliding dislocations with weak pinning solute atoms all around the space, resulting in the two-thirds power dependence of strengthening on the solute concentration, which is applicable to the concentrated solid solutions.[12] A way to treat SSS of

a)Address all correspondence to this author.
e-mail: jsun@sjtu.edu.cn
DOI: 10.1557/jmr.2018.174

the multicomponent alloys was further proposed by Gypen and Deruyttere,[13] when the binary SSS caused by each of the solutes is known. Recently, studies of SSS in the binary Ni-based alloys, such as Ni–Fe, Ni–Mo, Ni–Co, and so on, by means of diffusion couples combined with nanoindentation showed that the two-thirds power dependence of hardness on the solute concentration predicted by the Labusch model is generally followed.[14–16] However, few studies of SSS have been reported up to now in the ternary Ni-based alloys.

Employing the Labusch theory to predict SSS, it is necessary to obtain information on the atomic and elastic misfit parameters of the alloys, which can be effectively calculated by using density functional theory (DFT). In this work, the compositional dependences of lattice parameters and elastic properties of the binary Ni–Co, Ni–Cr and ternary Ni–Co–Cr alloys have been investigated by using the exact muffin-tin orbitals (EMTO) method. The coherent potential approximation (CPA) has been used to describe the random distribution of the alloying atoms in the alloys. Based on the calculated results of lattice parameters and elastic properties, the SSS effect of these alloys was studied by using the Labusch theory. Particularly, the SSS model proposed by Gypen and Deruyttere[13] for the multicomponent solid solutions has been discussed for the ternary Ni–Co–Cr alloys.

## II. COMPUTATIONAL METHOD

First-principles calculations were performed by using the EMTO method based on DFT.[17–19] The EMTO method is an improved screened Korringa–Kohn–Rostoker (KKR) method,[20] where the one-electron potential is represented by large overlapping muffin-tin potential spheres. Generalized gradient approximation (GGA) parameterized by Perdew, Burke, and Ernzerhof (PBE) was used to treat the exchange-correlation density functional.[21] In the self-consistent calculations, the one-electron equations were solved within the soft core scheme and scalar-relativistic approximations. The Green's function was calculated for 16 complex energy points distributed exponentially on a semicircular contour, including states within 1 Ry below the Fermi level. The basis sets included $s$, $p$, $d$, and $f$ components. The Ni-$3p^6 4s^2 3d^8$, Co-$3p^6 4s^2 3d^7$, and Cr-$3p^6 4s^2 3d^4$ were treated as valence states. The irreducible parts of the Brillouin zones were sampled by uniformly distributed $k$-points. The $k$-points of $27 \times 27 \times 27$ were chosen for the fcc structure.

The disordered binary Ni–(5–30)Co and Ni–(5–25)Cr alloys and ternary Ni–(10–30)Co–(10–25)Cr alloys (in at.%) are described with the CPA[22] as implemented in the EMTO method. CPA is an efficient and useful approach to dispose the compositional and magnetic disorder in random solid-solution alloys. It is noteworthy that local atomic relaxations are neglected within the CPA method. Previous studies have demonstrated that the local lattice distortion has negligible effect on the equilibrium volume and elastic properties of solid solutions.[23] In the systems where the elements are similar in size, i.e., Fe–Cr,[24] Fe–Ni–Cr alloys,[25] and the multicomponent high entropy alloys,[26] the single-site CPA method has been successfully used to study the phase stability and elastic properties. In this work, these ternary Ni–Co–Cr alloys are considered to be ferromagnetic for their total energies of ferromagnetic ($E_{FM}$) states, which are smaller than those of paramagnetic ($E_{PM}$) states. The magnetic critical temperature (Curie temperature, $T_C$) can be estimated from the total energy difference, according to the equation $3k_B T_C = 2\,(E_{PM} - E_{FM})/(1 - c)$,[27] where $k_B$ is the Boltzmann constant and $c$ is the concentration of the nonmagnetic component. Since there is no nonmagnetic component in the alloys, $(1 - c)$ is set to 1. The paramagnetic state is described by the disordered local moments approach.[28] The estimated critical temperature ranges from 85 to 228 K for the ternary Ni–Co–Cr alloys. Therefore, the calculated results of the ternary ferromagnetic Ni–Co–Cr alloys are strictly valid at low temperature.

The fcc structure has three independent elastic constants $C_{11}$, $C_{12}$, and $C_{44}$. These elastic constants were calculated by volume-conserving distortions. The orthorhombic distortion was used to determine the tetragonal shear modulus $C' = (C_{11} - C_{12})/2$:

$$\begin{bmatrix} 1+\delta_o & 0 & 0 \\ 0 & 1-\delta_o & 0 \\ 0 & 0 & \frac{1}{1-\delta_o^2} \end{bmatrix} . \quad (1)$$

The energy change is expressed as

$$\Delta E(\delta_o) = 2VC'\delta_o^2 + O\left(\delta_o^4\right) \quad , \quad (2)$$

$$B = (C_{11} + C_{12})/3 \quad , \quad (3)$$

where $B$ is the bulk modulus calculated from the equation of state fitting the total energy against volume from the volume optimization. $C_{11}$ and $C_{12}$ were obtained from equations of $C' = (C_{11} - C_{12})/2$ and $B = (C_{11} + C_{12})/3$. The monoclinic distortion was used to determine $C_{44}$:

$$\begin{bmatrix} 1 & \delta_m & 0 \\ \delta_m & 1 & 0 \\ 0 & 0 & \frac{1}{1-\delta_m^2} \end{bmatrix} . \quad (4)$$

The energy change is given by

$$\Delta E(\delta_m) = 2VC_{44}\delta_m^2 + O(\delta_m^4) \quad , \tag{5}$$

where $\delta$ is the strain and five strains $\delta = 0.01$–$0.05$ were used for each distortion in the calculations. The polycrystalline shear modulus $G$ is derived from the single-crystal elastic constants using the Voigt–Reuss–Hill average method,[29]

$$G_H = (G_V + G_R)/2 \quad , \tag{6}$$

$$G_V = (C_{11} - C_{12} + 3C_{44})/5 \quad , \tag{7}$$

$$G_R = 5(C_{11} - C_{12})C_{44}/[4C_{44} + 3(C_{11} - C_{12})] \quad . \tag{8}$$

The Young's modulus $E$ and the Poisson ratio $\nu$ are connected to $B$ and $G$ by the relations of $E = 9BG/(3B + G)$ and $\nu = (3B - 2G)/(6B + 2G)$.

## III. RESULTS AND DISCUSSION

### A. Lattice parameters and magnetic moments

#### 1. Binary Ni–Co and Ni–Cr alloys

The ground state properties of the fcc Ni metal were first calculated, and the results are presented in Table I, in which other theoretical results and experimental data are also given for references. It can be seen from Table I that the lattice parameter of fcc Ni calculated by the EMTO method agrees well with the other theoretical results achieved by the projector augmented wave method (PAW)[30] and all-electron full-potential linear augmented plane wave method (FLAPW),[31] and experimental results in the literature.[32]

The calculated lattice parameters as a function of the Co and Cr concentrations in the binary Ni–(5–30)Co and Ni–(5–25)Cr alloys are shown in Figs. 1(a) and 1(b), respectively. The theoretical results are in good agreement with experimental data, with the typical level of error (~2%) for DFT lattice constants.[33,34] The different errors for the calculated lattice parameters of the Ni–Co and Ni–Cr alloys result from the exchange-correlation density functionals, for there is no universal gradient-level approximation, yielding a consistent error for transition metals and alloys. Recently, based on an element-specific optimization of the parameters in the exchange-correlation functionals, a concept of quasi-nonuniform gradient-level approximation was introduced for DFT calculations, and the theoretical lattice parameters and bulk moduli are in better agreement with the experimental results.[35,36] Both Co and Cr increase the lattice parameter linearly. The slope of the lattice parameters $\Delta a/\Delta x$ of the Ni–Co alloys is smaller than that of the Ni–Cr alloys by a factor of 3.7.

TABLE I. Theoretical and experimental lattice parameter $a$ (Å), elastic constants (GPa), elastic moduli (GPa), and Poisson's ratio ($\nu$) of pure Ni.

| $a$ | $C_{11}$ | $C_{12}$ | $C_{44}$ | $B$ | $G$ | $E$ | $\nu$ | |
|---|---|---|---|---|---|---|---|---|
| 3.522 | 260.9 | 164.3 | 150.7 | 196.5 | 95.6 | 246.9 | 0.291 | EMTO in this work |
| 3.522 | 275.5 | 160.1 | 126.3 | 198.6 | 92.2 | 239.6 | 0.299 | PAW[30] |
| 3.520 | 287.0 | 155.0 | 150.0 | 199.0 | 107.9 | 274.1 | 0.270 | FLAPW[31] |
| | 261.0 | 151.0 | 132.0 | 187.7 | 92.9 | 239.2 | 0.288 | 4 K[32] |
| 3.524 | 251.6 | 150.8 | 122.0 | 184.4 | 85.6 | 222.3 | 0.299 | 300 K[32] |

The total and local magnetic moments as a function of the Co and Cr concentrations in the Ni–Co and Ni–Cr alloys are presented in Figs. 2(a) and 2(b), respectively. The magnetic moments of Co and Ni [$\mu$(Co) and $\mu$(Ni)] show a very weak dependence on the Co concentration, which is in line with the experimental results.[37] The total magnetic moment increases linearly with increasing the Co concentration. In the Ni–Cr alloys, Ni and Cr atoms are antiferromagnetically coupled and the magnetic moments [$\mu$(Ni) and $\mu$(Cr)] decrease with the Cr concentration due to magnetic frustration.[38] Both magnetic moments vanish at 12.5Cr at.%. A similar compositional dependence of the magnetic moment was observed in the binary Fe–Cr alloys.[39]

#### 2. Ternary Ni–Co–Cr alloys

For the ternary Ni–(10–30)Co–(10–25)Cr alloys, all properties were actually calculated with a compositional interval of 2%. The calculated results were then used for plotting the contour figures. The calculated lattice parameters as a function of the Co and Cr concentrations in the ternary Ni–(10–30)Co–(10–25)Cr alloys are shown in Fig. 3. It can be seen that at various concentrations of Co, the lattice parameter always increases approximately linearly with Cr addition, with a larger slope of $\Delta a/\Delta x$ at lower Co concentration. However, Cr addition leads to a nonlinear dependence of the lattice parameter, that is, to say at low Cr concentration (~16 at.%), the lattice parameter almost monotonously increases with Co addition, while at high Cr concentration (~22 at.%), it decreases with Co addition. The maximum lattice parameter appears at the Ni–10Co–25Cr concentration. The equilibrium lattice parameters for Ni, Co, and Cr pure metals with the fcc structure are 3.52 Å, 3.53 Å, and 3.63 Å (equivalent to 2.96 Å in bcc Cr), respectively. Obviously, the calculated lattice parameters for the ternary alloys do not follow the linear rule of mixing (Vegard's law). To understand this, it is recalled that the experimental slopes of the lattice parameters $\Delta a/\Delta x$ for $Ni_{1-x}Co_x$, $Ni_{1-x}Cr_x$, and $Cr_{1-x}Co_x$ systems are $0.2 \times 10^{-3}$ Å/at.%,[33] $1.2 \times 10^{-3}$ Å/at.%,[33] and $-2.1 \times 10^{-3}$ Å/at.%,[40] respectively. The variations in the lattice parameters of the ternary $Ni_{1-x-y}Co_xCr_y$ alloys when the Cr concentration is fixed and Ni is replaced by

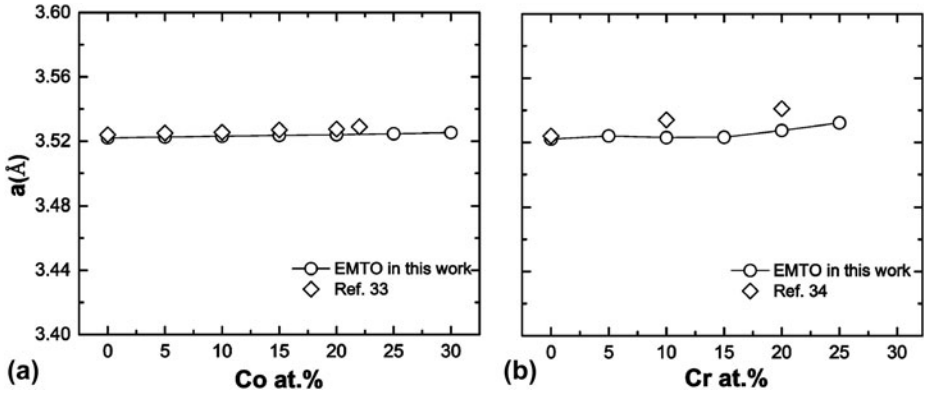


FIG. 1. Dependence of lattice parameters on (a) Co content in Ni–Co alloys and (b) Cr content in Ni–Cr alloys.

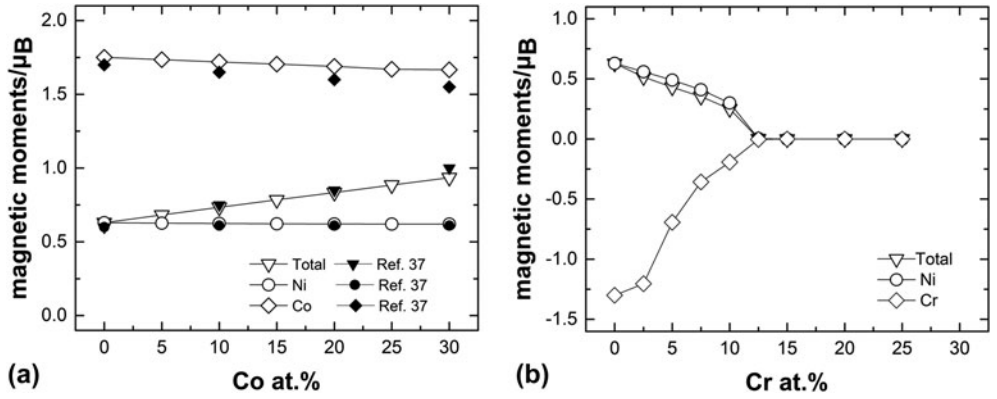


FIG. 2. Dependence of total and local magnetic moments on (a) Co content in Ni–Co alloys and (b) Cr content in Ni–Cr alloys.

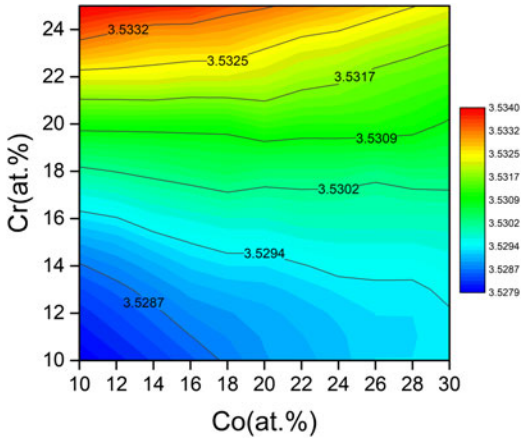


FIG. 3. Contour plot of compositional dependence of lattice parameters of the ternary Ni–Co–Cr alloys.

Co may be approximated by three respective binary systems via $(1 - y)Ni_{1-z}Co_z + y(Ni_{1-z}Cr_z + Cr_{1-z}Co_z)$, where the interaction coefficients of different pairs of atoms are assumed to be the weight factor $1 - y$ and $y$, respectively.[41] Thus, the slopes of the lattice parameters $\Delta a/\Delta x$ are estimated as $\delta(Ni_{1-x-0.1}Co_xCr_{0.1}) = 1.0 \times 10^{-3}$ Å/at.%, $\delta(Ni_{1-x-0.18}Co_xCr_{0.18}) = 0.02 \times 10^{-3}$ Å/at.%, $\delta(Ni_{1-x-0.2}Co_xCr_{0.2}) = -0.02 \times 10^{-3}$ Å/at.%, and $\delta(Ni_{1-x-0.25}Co_xCr_{0.25}) = -0.075 \times 10^{-3}$ Å/at.%, which are in line with the calculated results presented in Fig. 3. This indicates that it is important to consider the Cr–Co chemical interactions on the lattice parameters of the ternary Ni–Co–Cr alloys when Cr concentration is high.

The total and local magnetic moments as a function of the Co and Cr concentrations in the ternary Ni–(10–30) Co–(10–25)Cr alloys are shown in Figs. 4(a)–4(d), respectively. The Ni moment μ(Ni) increases mildly with Co addition but decreases markedly with Cr addition. μ(Co) depends weakly on the Co concentration, similar to that in the Ni–Co alloys, but decreases significantly with Cr addition. μ(Cr) decreases with Co addition but increases with Cr addition. As a result, the total magnetic moment in the ternary Ni–(10–30)Co–(10–25)Cr alloys increases markedly with Co addition while decreases with Cr addition.

## B. Elastic constants and moduli

### 1. Binary Ni–Co and Ni–Cr alloys

As shown in Table I, the elastic constants of fcc Ni from the present EMTO calculations are in reasonable agreement with those from other theoretical

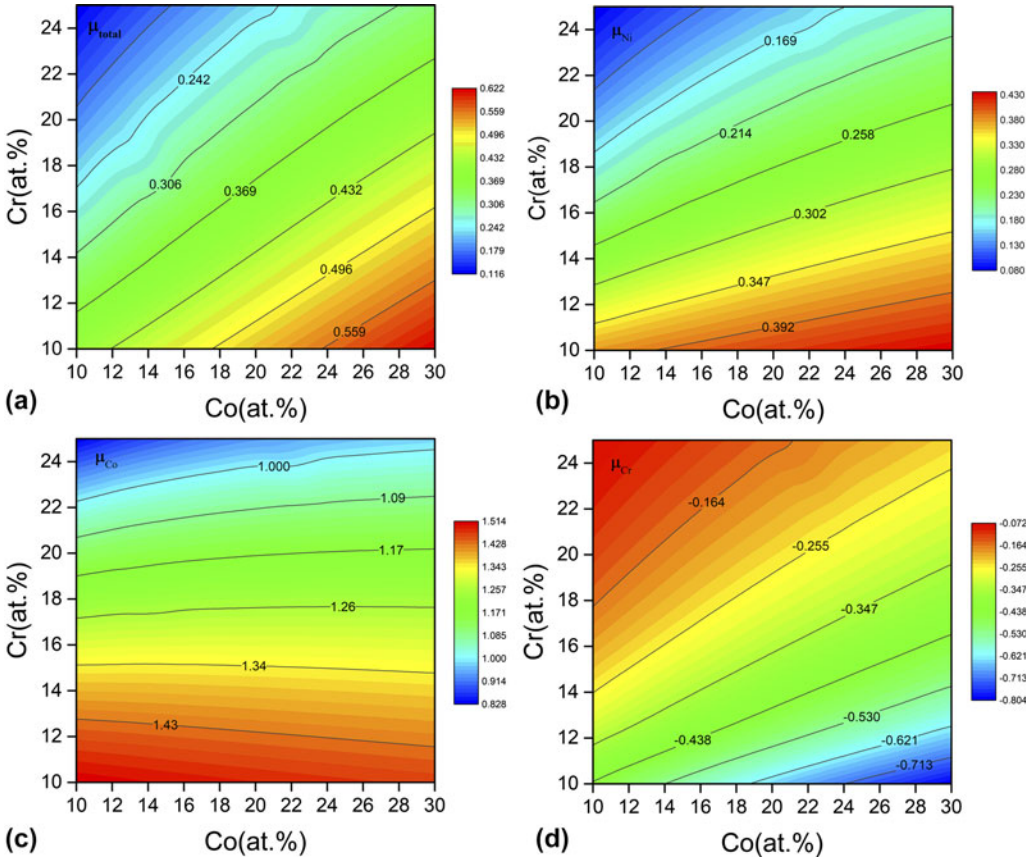


FIG. 4. Contour plot of compositional dependence of total (a) μ(total), and local magnetic moments (b) μ(Ni), (c) μ(Co), and (d) μ(Cr) of the ternary Ni–Co–Cr alloys.

calculations[30,31] and from experimental measurements,[32] except that the elastic constant $C_{44}$ is somewhat overestimated (The deviation still falls into the typical range of error for the DFT elastic constants). The polycrystal elastic moduli of fcc Ni from the present EMTO calculations also agree reasonably with those in the literature.[30–32]

The calculated elastic constants as a function of the Co and Cr concentrations in the Ni–Co and Ni–Cr alloys are presented in Figs. 5(a)–5(f), respectively. All the elastic constants increase mildly with an increase in the Co and Cr concentrations in the Ni–Co and Ni–Cr alloys, respectively. The calculated elastic constants of Ni–10Co, Ni–25Co, and Ni–20Cr alloys are overestimated in comparison with the experimental values of Ni–10.1Co and Ni–26.35Co alloys by less than 15%[42] and of the Ni–19.6Cr alloy by about 20%.[43] In general, there are two sources of error for the DFT elastic constants. The first part of the error comes from the neglect of thermal and zero-point vibration in the present calculations. The second error arises from the exchange-correlation density functionals[35,36] discussed above. As shown in Figs. 1(a) and 1(b), the EMTO calculations underestimate the lattice parameters of the Ni–Co and Ni–Cr alloys, leading to overestimation of the elastic constants. Although there is deviation between the calculated elastic constants and experimental ones, this deviation does not affect the trend of compositional dependence of elastic properties for the Ni–Co and Ni–Cr alloys. The bulk, shear, and Young's moduli ($B$, $G$, and $E$) as a function of the Co and Cr concentrations in the Ni–Co and Ni–Cr alloys are presented in Figs. 6(a)–6(f), respectively. For the Ni–Co alloys, they all slightly increase with the Co concentration. For the Ni–Cr alloys, the bulk modulus increases, and the shear and Young's moduli decrease with the Cr concentration. The theoretical compositional dependence of the Young's modulus agrees with the experimental results for both Ni–Co and Ni–Cr alloys.[7]

## 2. Ternary Ni–Co–Cr alloys

The calculated elastic constants of the ternary Ni–(10–30)Co–(10–25)Cr alloys as a function of composition are plotted in Figs. 7(a)–7(c). It is seen that $C_{11}$ increases with Cr addition at various Co concentrations and with Co addition at high Cr concentration. $C_{11}$ is weakly dependent on the Co addition at low Cr

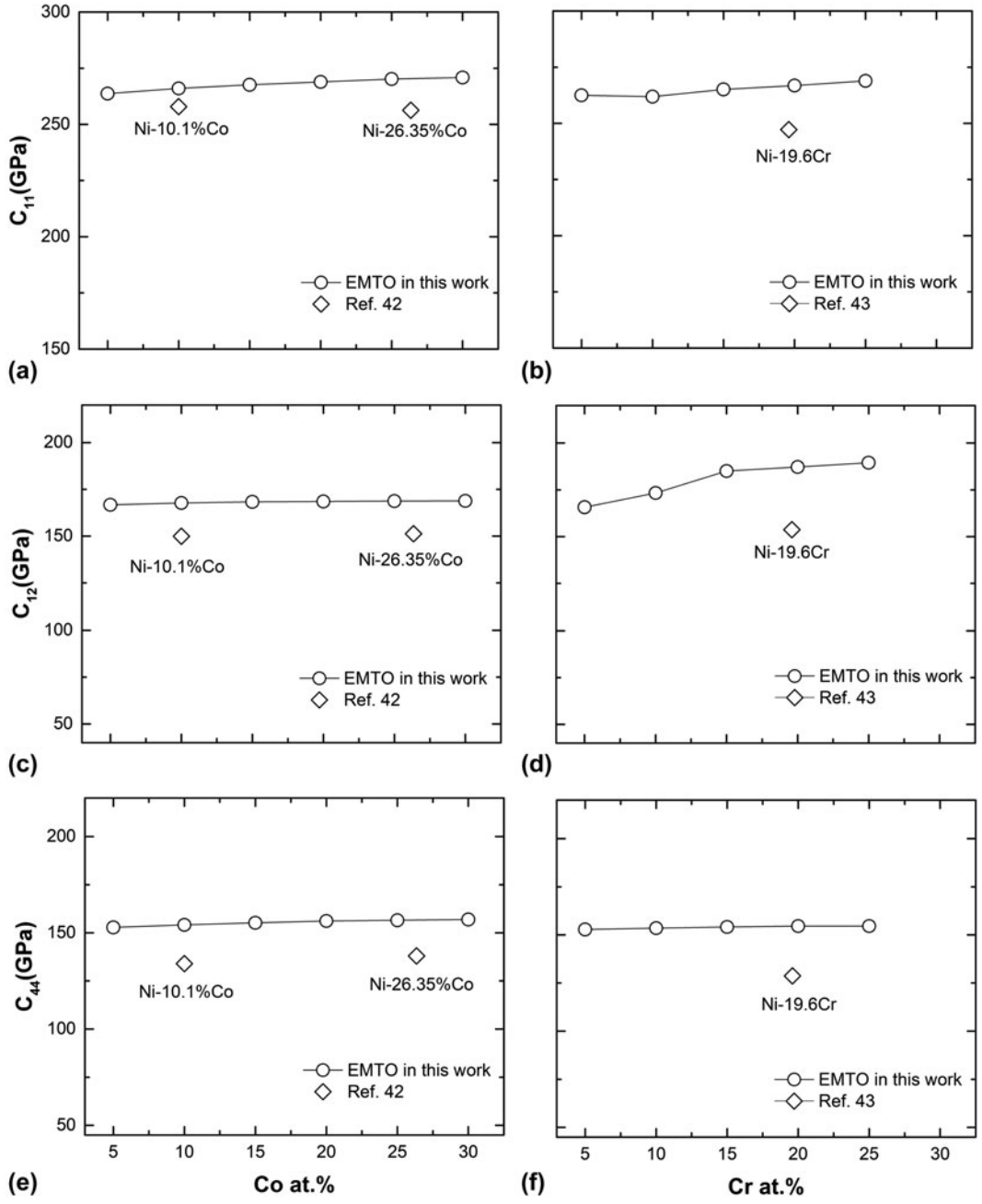


FIG. 5. Dependence of elastic constants (a, c, and e) on Co content in Ni–Co alloys and (b, d, and f) on Cr content in Ni–Cr alloys.

concentration. The maximum $C_{11}$ occurs at high Cr and Co concentrations [Fig. 7(a)]. $C_{12}$ increases with Cr addition, especially at low Co concentration, while $C_{12}$ decreases with Co addition [Fig. 7(b)]. $C_{44}$ increases with both Cr and Co additions, and the maximum $C_{44}$ is located at high Cr and Co concentrations [Fig. 7(c)]. The overall variations of $C_{11}$, $C_{12}$, and $C_{44}$ as a function of composition are relatively small. The elastic moduli and Poisson's ratio of the ternary Ni–(10–30)Co–(10–25)Cr alloys as a function of composition are plotted in Figs. 8(a)–8(e). The bulk modulus increases with Cr addition but decreases with Co addition. The maximum $B$ appears at the Ni–10Co–25Cr concentration [Fig. 8(a)]. On the contrary, the shear modulus decreases with Cr addition but increases with Co addition. The maximum $G$ occurs at the Ni–30Co–10Cr concentration [Fig. 8(b)]. The Young's modulus has a similar compositional dependence as that of the shear modulus [Fig. 8(c)]. The ratio of $B$ and $G$ is often used to evaluate the ductile/brittle behavior of the alloys. According to Pugh's approximation, the material is ductile when its $B/G$ is larger than 1.75; otherwise, it is brittle.[44] For the studied compositional range, all $B/G$

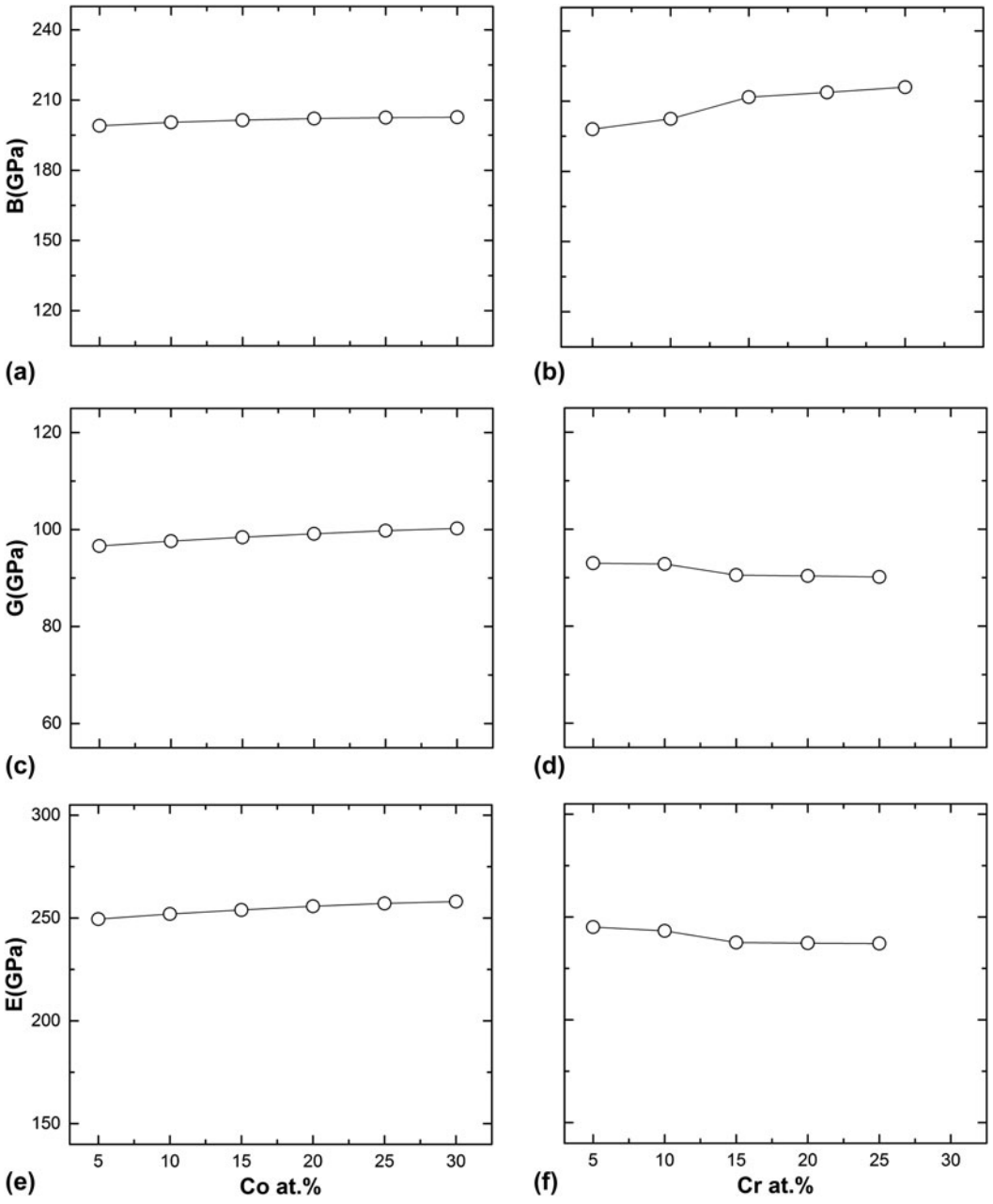


FIG. 6. Dependence of elastic moduli (a, c, and e) on Co content in Ni–Co alloys and (b, d, and f) on Cr content in Ni–Cr alloys.

values for the ternary Ni–(10–30)Co–(10–25)Cr alloys are larger than 1.75, indicating that the alloys are ductile. They show a similar compositional dependence as the bulk modulus [Fig. 8(d)]. Poisson's ratios, ν, of the ternary Ni–(10–30)Co–(10–25)Cr alloys were also calculated, showing a similar compositional dependence as $B/G$ [Fig. 8(e)].

## C. SSS

### 1. Binary Ni–Co and Ni–Cr alloys

According to Labusch,[12] the additional strength resulting from SSS for a solute atom $i$ can be expressed as

$$\Delta\tau = B_i C_i^{2/3} \quad , \tag{9}$$

$$B_i = 3G\varepsilon^{4/3} Z \quad , \tag{10}$$

where $B_i$ is the strengthening parameter, corresponding to the experimental hardening rate of $k$. $Z$ is a constant independent of the solute atom. $G$ is the shear modulus of the matrix. $C_i$ is the atomic fraction of the solute atoms. ε and $\eta'$ are the Fleischer parameter and modulus interaction term, which are expressed by

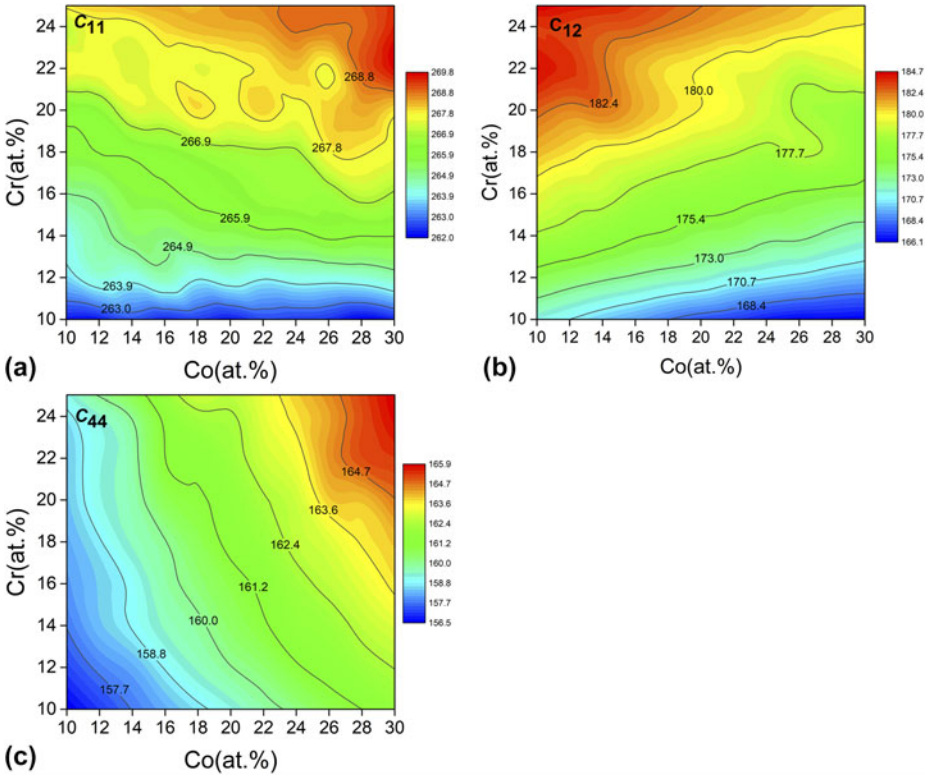


FIG. 7. Contour plot of compositional dependence of elastic constants (a) $C_{11}$, (b) $C_{12}$, and (c) $C_{44}$ of the ternary Ni–Co–Cr alloys.

$$\varepsilon = \left(\eta'^2 + \alpha^2\delta^2\right)^{1/2} \quad , \tag{11}$$

$$\eta' = \eta/(1 + 0.5|\eta|) \quad . \tag{12}$$

Here, $\eta$ and $\delta$ are the modulus and atomic misfit parameters, which are given by

$$\eta = \frac{1}{G}\left(\frac{\partial G}{\partial C}\right) \quad , \tag{13}$$

$$\delta = \frac{1}{a}\left(\frac{\partial a}{\partial C}\right) \quad , \tag{14}$$

where $\alpha$ is the constant ($3 < \alpha < 16$) for the interaction between solute atoms and screw dislocations ($\alpha$ is usually assumed to be 16 for fcc-structured alloys) and $a$ is the lattice constant. Using the lattice parameters and shear moduli shown in Figs. 1 and 6, the average strengthening parameters were calculated to be 31.35 MPa/at.%$^{2/3}$ for the Ni–Co and 85.73 MPa/at.%$^{2/3}$ for the Ni–Cr alloys, respectively. It can be seen that both Co and Cr additions result in a distinct SSS for the Ni–Co and Ni–Cr alloys, respectively, and the SSS effect of Cr is stronger than that of Co by a factor of 2.7 because the atomic misfit parameter of the Ni–Cr alloys is larger than that of the Ni–Co alloys. This indicates that the SSS is governed by the atomic misfit parameter, and the contribution of the modulus misfit parameter is small. The average strengthening parameter is close to the experimental result of 96.8 MPa/at.%$^{2/3}$ for the Ni–Cr alloys,[9,15] while for the Ni–Co alloys, the average strengthening parameter is smaller than the experimental value of 54.9 MPa/at.%$^{2/3}$.[10,15] The reason could be ascribed to the contribution of stacking faults to SSS in the Ni–Co alloys. It was claimed that Co addition decreases dramatically the stacking fault energies in the Ni–Co alloys,[10] leading to additional strengthening through the suppression of cross-slip mediated deformation.

## 2. Ternary Ni–Co–Cr alloys

According to Gypen and Deruyttere,[13] the additional strength resulting from SSS for the multicomponent alloys can be expressed as

$$\Delta\tau = \left(\sum_i B_i^{3/2} C_i\right)^{2/3} \quad . \tag{15}$$

Using the lattice parameters and shear moduli of the binary Ni–Co and Ni–Cr alloys shown in Figs. 1 and 6, the compositional dependence of SSS in the ternary Ni–(10–30)Co–(10–25)Cr alloys was calculated, as

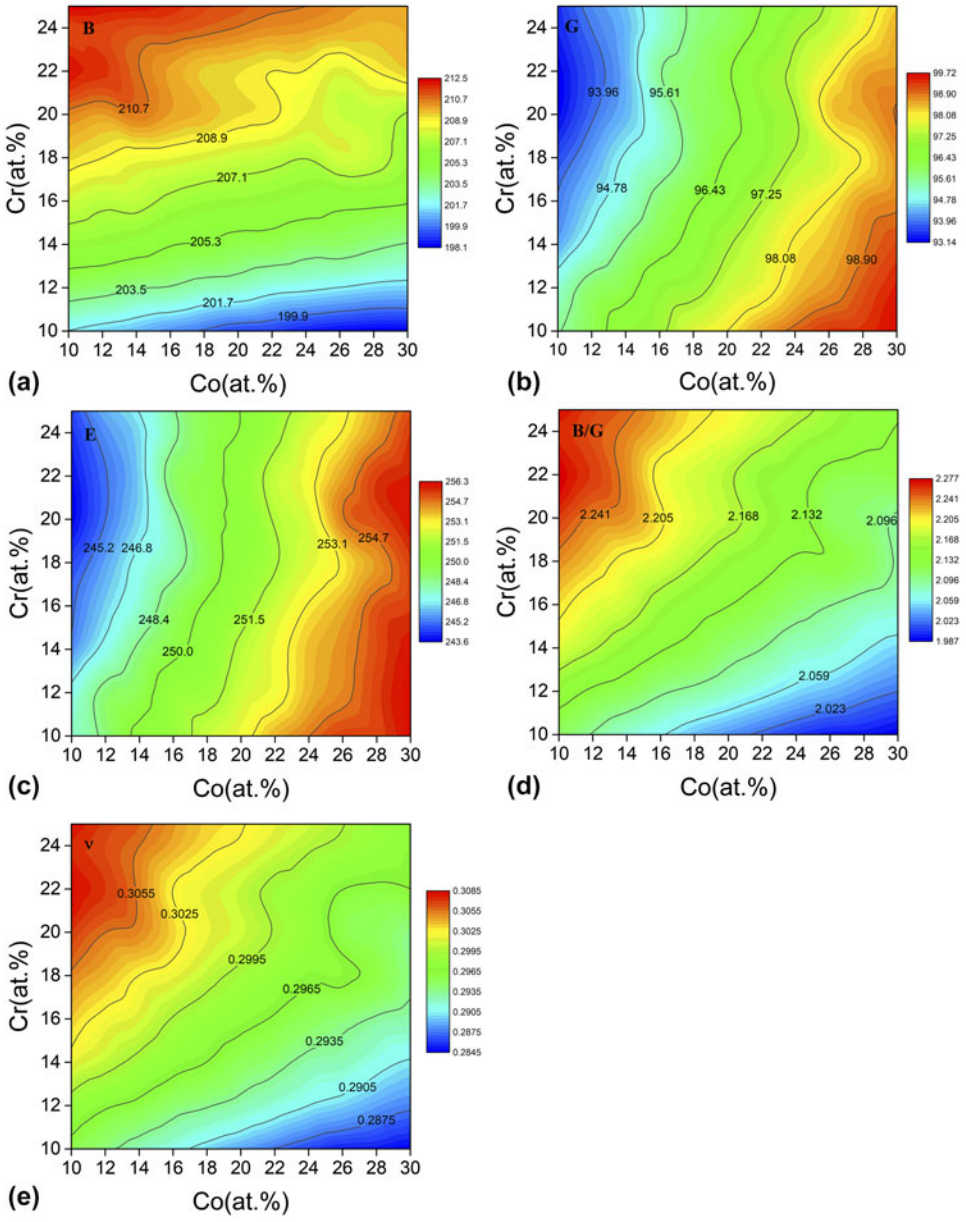


FIG. 8. Contour plot of compositional dependence of elastic moduli (a) *B*, (b) *G*, (c) *E*, (d) *B*/*G*, and (e) ν of the ternary Ni–Co–Cr alloys.

shown in Fig. 9(a). It is seen from Fig. 9(a) that SSS increases linearly with both Co and Cr concentrations, and the maximum SSS effect is found at the Ni–30Co–25Cr concentration.

It is noteworthy that in Eq. (15), the calculated SSS effect for the ternary Ni–Co–Cr alloys arises only from the contributions of the binary Ni–Co and Ni–Cr systems, but not from the Co–Cr system. As a matter of fact, present calculations have shown that the lattice parameters are related to the interactions among the Ni–Co, Ni–Cr and Co–Cr systems for the ternary Ni–Co–Cr concentrated alloys. Therefore, the SSS model proposed by Gypen and Deruyttere[13] for the multicomponent solid solutions may not apply to the ternary Ni–Co–Cr concentrated alloys. To fully account the SSS effect in the ternary alloys, the lattice parameters and shear moduli of the ternary alloys shown in Figs. 3 and 8 are used to calculate the related parameters in Eqs. (11) and (12) for the ternary Ni–(10–30)Co–(10–25)Cr alloys, where Co and Cr are treated as the "effective solute" and Ni as the solvent as suggested in Ref. 45. The atomic and modulus misfit parameters in Eqs. (11) and (12) are expressed as

$$\delta = \frac{a_{\mathrm{Ni}_{1-x-y}\mathrm{Co}_x\mathrm{Cr}_y} - a_{\mathrm{Ni}}}{(1 - C_{\mathrm{Ni}})a_{\mathrm{Ni}}} \quad , \tag{16}$$

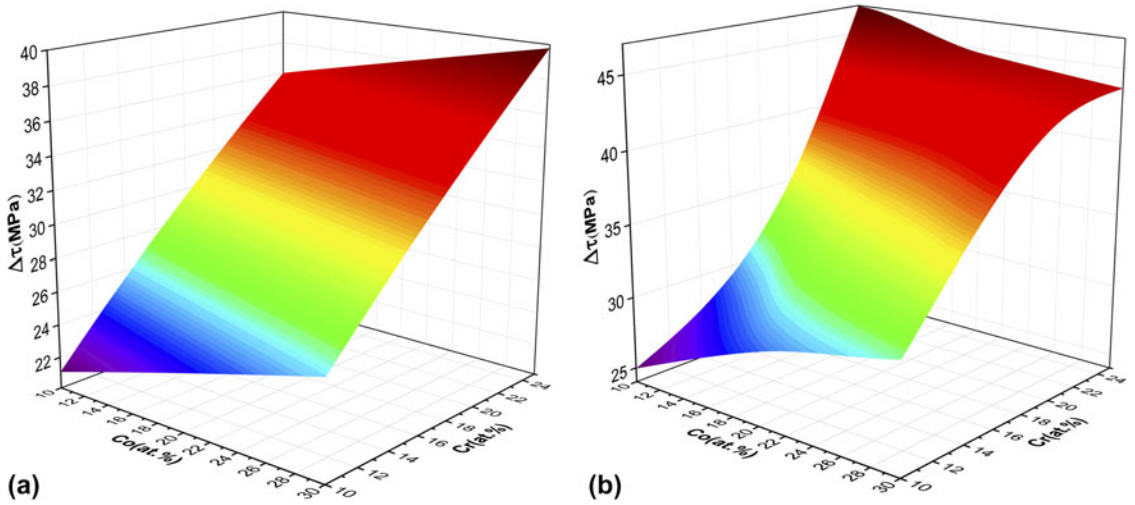


FIG. 9. Solid-solution strengthening (a) from the model in the literature[13] and (b) from revised model in this work for the ternary Ni–Co–Cr alloys.

$$\eta = \frac{G_{\mathrm{Ni}_{1-x-y}\mathrm{Co}_x\mathrm{Cr}_y} - G_{\mathrm{Ni}}}{(1 - C_{\mathrm{Ni}})G_{\mathrm{Ni}}} \quad . \tag{17}$$

The SSS effect for the ternary Ni–(10–30)Co–(10–25)Cr alloys is then calculated according to Eqs. (9) and (10). The compositional dependence of SSS of the ternary Ni–(10–30)Co–(10–25)Cr alloys is shown in Fig. 9(b), in which a larger SSS effect is observed compared to the results in Fig. 9(a). Furthermore, a different compositional dependence of SSS is revealed. At fixed Co concentrations, SSS always increases with Cr addition. While the effect of Co on SSS depends strongly on the actual Cr concentration, i.e., at low Cr concentration, SSS mildly increases with Co addition, which is in accordance with that from the model proposed by Gypen and Deruyttere,[13] but at high Cr concentration, it slightly decreases with the increasing Co concentration due to the Cr–Co chemical interactions.

Co and Cr are the main alloying elements partitioning preferentially in the γ phase of the Ni-based superalloys.[3–5] The present work shows that the addition of Co and Cr produces a significant SSS in the matrix of the Ni-based superalloys. With the DFT results of compositional dependence of SSS, the alloy composition is able to be optimized to improve the mechanical properties of the Ni-based superalloys.

## IV. SUMMARY

The elastic properties and SSS of the binary Ni–(5–30) Co and Ni–(5–25)Cr and ternary Ni–(10–30)Co–(10–25)Cr (at.%) solid-solution alloys have been investigated using the EMTO–CPA method. The calculated results are summarized as follows:

(1) Both Co and Cr increase the lattice parameters of the binary alloys linearly. The slope of the lattice parameter $\Delta a/\Delta x$ of the Ni–Co alloys is smaller than that of the Ni–Cr alloys by a factor of 3.7. However, nonlinearity is found in the compositional dependence of the lattice parameter in the ternary Ni–Co–Cr alloys, i.e., Co increases and decreases the lattice parameter at low and high Cr concentrations, respectively, which emphasizes the effect of chemical interactions among alloying elements on the lattice parameter.

(2) The total magnetic moment increases with increasing the Co concentration for the Ni–Co alloys while decreases markedly with increasing the Cr concentration and reaches zero at 12.5Cr at.% for the Ni–Cr alloys. In the ternary Ni–Co–Cr alloys, the total magnetic moments increase markedly with Co addition but decrease with Cr addition.

(3) The bulk, shear, and Young's moduli of the Ni–Co alloys increase with Co addition. The bulk modulus increases, while the shear and Young's moduli decrease with Cr addition in the Ni–Cr alloys. The bulk modulus increases with Cr addition while decreases with Co addition in the ternary Ni–Co–Cr alloys. On the contrary, the shear and Young's moduli decrease with Cr addition but increase with Co addition.

(4) Both Co and Cr additions result in effective SSS for the Ni–Co and Ni–Cr alloys, and Cr addition has a larger effect. In the ternary alloys, SSS increases significantly with Cr addition and mildly with Co addition at low Cr concentration but decreases with Co addition at high Cr concentration in the ternary Ni–Co–Cr alloys. For the present Ni–Co–Cr concentrated alloys, the model proposed by Gypen and Deruyttere may not be enough.

## ACKNOWLEDGMENTS

This research is supported by the National Key R&D Program of China (Project No. 2016YFB0701405) and the Science and Technology Committee of Shanghai Municipal (Project No. 14521100601).

## REFERENCES

1. R.C. Reed: *The Superalloys* (Cambridge University Press, Cambridge, England, 2006).
2. C.T. Sims, N.S. Stoloff, and W.C. Hagel: *Superalloys II* (John Wiley, New York, 1987); p. 97.
3. M.R. Jahangiri, H. Arabi, and S.M.A. Boutorabi: Development of wrought precipitation strengthened IN939 superalloy. *Mater. Sci. Eng.* **28**, 1470 (2012).
4. E. Fleischmann, M.K. Miller, E. Affeldt, and U. Glatzel: Quantitative experimental determination of the solid solution hardening potential of rhenium, tungsten and molybdenum in single-crystal nickel-based superalloys. *Acta Metall* **87**, 350 (2015).
5. Y. Gu, H. Harada, C. Cui, D. Ping, A. Sato, and J. Fujioka: New Ni–Co-base disk superalloys with higher strength and creep resistance. *Scrip Metall* **55**, 815 (2006).
6. K.A. Christofidou, N.G. Jones, M.C. Hardy, and H.J. Stone: The oxidation behaviour of alloys based on the Ni–Co–Al–Ti–Cr system. *Oxid. Met.* **85**, 443 (2016).
7. Y. Mishima, S. Ochiai, N. Hamao, M. Yodogawa, and T. Suzuki: Solid solution hardening of nickel-role of transition metal and B-subgroup solutes. *Trans. Japan Inst. Met.* **27**, 656 (1986).
8. H.A. Roth, C.L. Davis, and R.C. Thomson: Modeling solid solution strengthening in nickel alloys. *Metall. Mater. Trans. A* **28**, 1329 (1997).
9. C.K.L. Davies, V. Sagar, and R.N. Stevens: The effect of the stacking fault energy on the plastic deformation of polycristalline NiCo-alloys. *Acta Metall.* **21**, 1343 (1973).
10. A. Akhtar and E. Teghtsoonian: Plastic deformation of Ni–Cr single crystal. *Metall. Trans.* **2**, 2757 (1971).
11. R.L. Fleischer: Substitutional solution hardening. *Acta Metall.* **11**, 203–209 (1963).
12. R. Labusch: A statistical theory of solid solution hardening. *Phys. Status Solidi* **41**, 659 (1970).
13. L.A. Gypen and A. Deruyttere: Multi-component solid solution hardening. *J. Mater. Sci.* **12**, 1028 (1977).
14. S.B. Kadambi, V.D. Divya, and U. Ramamurty: Evaluation of solid-solution hardening in several binary alloy systems using diffusion couples combined with nanoindentation. *Metall. Mater. Trans. A* **48**, 4574 (2017).
15. O. Franke, K. Durst, and M. Göken: Nanoindentation investigations to study solid solution hardening in Ni-based diffusion couples. *J. Mater. Res.* **24**, 1127 (2009).
16. J.C. Zhao: A combinatorial approach for efficient mapping of phase diagrams and properties. *J. Mater. Res.* **16**, 1565 (2001).
17. L. Vitos, I.A. Abrikosov, and B. Johansson: Anisotropic lattice distortions in random alloys from first principles theory. *Phys. Rev. Lett.* **87**, 156401 (2001).
18. L. Vitos: Total-energy method based on the exact muffin-tin orbitals theory. *Phys. Rev. B* **64**, 167 (2001).
19. P. Hohenberg and W. Kohn: Inhomogeneous electron gas. *Phys. Rev. B* **136**, 864 (1964).
20. O.K. Andersen, O. Jepsen, and G. Krier: Exact Muffin-Tin Orbital Theory. In *Lectures on Methods of Electronic Structure Calculations*, edited by V. Kumar, O.K. Andersen, and A. Mookerjee (World Scientific, Singapore, 1994); p. 63.
21. J.P. Perdew, K. Burke, and M. Ernzerhof: Generalized gradient approximation made simple. *Phys. Rev. Lett.* **77**, 3865 (1996).
22. B. Gyorffy: Coherent potential approximation for a nonoverlapping muffin-tin potential model of random substitutional alloys. *Phys. Rev. B* **5**, 2382 (1972).
23. L.Y. Tian, G. Wang, J.S. Harris, D.L. Irving, J. Zhao, and L. Vitos: Alloying effect on the elastic properties of refractory high-entropy alloys. *Mater. Des.* **114**, 243 (2017).
24. P. Olsson, I.A. Abrikosov, L. Vitos, and J. Wallenius: Ab initio formation energies of Fe–Cr alloys. *J. Nucl. Mater* **321**, 84 (2003).
25. L. Vitos, P.A. Korzhavyi, and B. Johansson: Stainless steel optimization from quantum mechanical calculations. *Nat. Mater* **2**, 25 (2003).
26. F. Tian, L. Delczeg, N. Chen, L.K. Varga, J. Shen, and L. Vitos: Structural stability of $NiCoFeCrAl_x$ high-entropy alloy from ab initio theory. *Phys. Rev. B* **88**, 085128 (2013).
27. D. Ma, B. Grabowski, F. Körmann, J. Neugebauer, and D. Raabe: Ab initio thermodynamics of the CoCrFeMnNi high entropy alloy: Importance of entropy contributions beyond the configurational one. *Acta Mater.* **100**, 90 (2015).
28. B.L. Győrffy, A.J. Pindor, J. Staunton, G.M. Stocks, and H. Winter: A first-principles theory of ferromagnetic phase transitions in metals. *J. Phys. F Met. Phys.* **15**, 1337 (1985).
29. R. Hill: The elastic behavior of a crystalline aggregate. *Proc. Phys. Soc., London, Sect. A* **65**, 349 (1952).
30. S.L. Shang, A. Saengdeejing, Z.G. Mei, D.E. Kim, H. Zhang, S. Ganeshan, Y. Wang, and Z.K. Liu: First-principles calculations of pure elements: Equations of state and elastic stiffness constants. *Comput. Mater. Sci* **48**, 813 (2010).
31. G.Y. Guo and H.H. Wang: Gradient-corrected density functional calculation of elastic constants of Fe, Co, and Ni in bcc, fcc, and hcp structures. *Chin. J. Phys.* **38**, 949 (2000).
32. H.M. Ledbetter and R.P. Reed: Elastic properties of metals and alloys, I. Iron, nickel, and iron–nickel alloys. *J. Phys. Chem. Ref. Data* **2**, 531 (1973).
33. W.B. Pearson and L.T. Thompson: The lattice spacings of nickel solid solutions. *Can. J. Phys* **35**, 349 (1957).
34. A. Taylor and R.W. Floyd: The constitution of nickel-rich alloys of the nickel chromium titanium system. *J. Inst. Metals* **80**, 577 (1952).
35. H. Levämäki, M.P.J. Punkkinen, K. Kokko, and L. Vitos: Quasi-non-uniform gradient-level exchange-correlation approximation for metals and alloys. *Phys. Rev. B* **86**, 201104 (2012).
36. H. Levämäki, M.P.J. Punkkinen, K. Kokko, and L. Vitos: Flexibility of the quasi-non-uniform exchange-correlation approximation. *Phys. Rev. B* **89**, 115107 (2014).
37. J. Kudrnovský, V. Drchal, and P. Bruno: Magnetic properties of fcc Ni-based transition metal alloys. *Phys. Rev. B* **77**, 224422 (2008).
38. M. Punkkinen, S. Kwon, J. Kollár, B. Johansson, and L. Vitos: Compressive surface stress in magnetic transition metals. *Phys. Rev. Lett.* **106**, 057202 (2011).
39. P. Olsson, I.A. Abrikosov, and J. Wallenius: Electronic origin of the anomalous stability of Fe-rich bcc Fe–Cr alloys. *Phys. Rev. B* **73**, 104416 (2006).
40. N. Yukawa, M. Hida, T. Imura, Y. Mizuno, and M. Kawamura: Structure of chromium-rich Cr–Ni, Cr–Fe, Cr–Co, and Cr–Ni–Fe alloy particles made by evaporation in argon. *Metall. Mater. Trans. B* **3**, 887 (1972).

41. E. Nurmi, G. Wang, K. Kokko, and L. Vitos: Assessing the elastic properties and ductility of Fe–Cr–Al alloys from ab initio calculations. *Philos. Mag. Ser.* **96**, 122 (2016).
42. H.J. Leamy and H. Warlimont: The elastic behaviour of Ni–Co alloys. *Phys Status Solidi. B* **37**, 523 (1970).
43. J.T. Lenkkeri: Measurements of elastic moduli of face-centred cubic alloys of transition metals. *J. Phys. F: Metal Phys* **11**, 1991 (1981).
44. S.F. Pugh: Relations between the elastic moduli and the plastic properties of polycrystalline pure metals. *Philos. Mag. Ser* **7**, 823 (1954).
45. Z. Wu, Y. Gao, and H. Bei: Thermal activation mechanisms and Labusch-type strengthening analysis for a family of high-entropy and equiatomic solid-solution alloys. *Acta Mater* **120**, 108 (2016).